Development of a high-performance immunolatex based on "soft landing" antibody immobilization mechanism

Xiaofei Yuan[1,2,3], Dolça Fabregat[5], Keitaro Yoshimoto[2] and Yukio Nagasaki[1,2,3,4*]

[1]Department of Materials Sciences, Graduate School of Pure and Applied Sciences, University of Tsukuba; [2]Tsukuba Advanced Research Alliance (TARA), and [3]Master School of Medical Sciences, Graduate School of Comprehensive Human Sciences, University of Tsukuba; [4]Satellite Laboratory of International Center for Materials Nanoarchitectonics (MANA) in National Institute for Materials Science (NIMS), University of Tsukuba, Tennodai 1−1−1, Tsukuba, Ibaraki 305-8573, Japan; and [5]Biokit Latex R&D Department, 08186 Lliçà d'Amunt, Barcelona, Spain.

[*]To whom correspondence should be addressed.

Tel: +81-29-853-5749; Fax: +81-29-853-5749; E-mail:yukio@nagalabo.jp

Abstract: Rabbit anti-human ferritin (anti-hFT) polyclonal immunoglobulin G (IgG) and poly(ethylene glycol) (PEG) were sequentially co-immobilized onto polystyrene submicroparticles (sMPs) to construct sMP/anti-hFT/PEG (SAP) immunolatex. Chemical immobilization of anti-hFT was performed at different pH levels to evaluate variations in antigen recognition. Basic pH disfavored conjugation of anti-hFT to sMPs, but remarkably increased its antigen recognition in comparison to that at neutral pH. We investigated this

intriguing phenomenon further by assessing the kinetics of antibody binding, including the time-dependency of immobilization, antigen recognition, and orientation of bound anti-hFT. Therefore, we attributed high antigen recognition to significant electrostatic repulsion between sMPs and anti-hFT at basic pH, which predominately prevented anti-hFT access to sMPs and concurrently promoted anti-hFT orientations suitable for antigen recognition. Subsequent PEG modification maintained such anti-hFT orientation, without which antigen-accessible orientations would have decreased with time. Thus, properly oriented antibody and immediate PEGylation after antibody immobilization contributed to the formation of a high-performance SAP immunolatex.

Keywords: Antibody immobilization, Antibody orientation, PEGylation, Immunolatex, Immunoassay, Immunoreactivity

1. Introduction

With the development of biotechnology and nanotechnology, immobilized proteins, especially antibodies and enzymes, have been widely used as biosensors [1], microarrays [2-5], and immunoparticles [6-8]. These applications require immobilized proteins to maintain their conformation and proper active site orientation toward the bulk solution. Protein immobilization, however, is a complicated process, mainly owing to the unique structural features of proteins, such as diversity, flexibility, and amphiphilic surface, thereby making the process difficult to control.

Antibody immobilization consists of physical adsorption and chemical binding, which depends on the driving force. The former is simple, but nonspecific attractive forces easily cause antibody desorption [9]. Chemical binding was proposed as a solution because stable covalent linkages with antibodies are formed. However, it likely results in random antibody conjugation, accompanied by reduced antigen recognition and/or denaturation [10,11]. Accordingly, controllable covalent binding with proper antibody orientation is crucial for desirable antibody immobilization. To date, much effort has been devoted to this challenging task. Several traditional methods have been developed, such as disulfide bonds at the constant moiety (Fc region) of IgG antibodies [12,13], site-specific modification of carbohydrates in the Fc region [14], acid pretreatment promoting the preferential Fc adsorption [15-17], and attachment via Fc-recognizing protein A [18] or protein G [19]. Use of these methods has resulted in some success in manipulating antibody orientation for efficient antibody–antigen interactions. From the viewpoint of industrial applications, however, all these strategies are still economically unfeasible because of complexity and length, coupled with the laborious procedures and special techniques involved in these strategies.

Versatile driving forces work during antibody physisorption, dependending on the features of antibodies and substrates [20-23], and the electrostatic interaction between them is one of the most important forces. Previous studies have shown that both the amount of immobilized antibodies and their orientation are affected by electrostatic interactions [21,22,24,25].

Simulation of antibody adsorption and orientation on a charged surface was also performed to support this kind of orientation control [23]. Even with chemical binding, the orientation of an antibody may be dramatically influenced by its physisorption properties. These properties are dependent on the substrate, because antibodies generally need to undergo physisorption prior to covalent conjugation [26]. We predict that controlling the interaction between antibodies and the substrate surface, by charging character of solid surface with proper pH, ionic strength, etc., may easily adjust the orientation of the antibody during chemical binding. Thus, combining physical orientation control with robust chemical linkage between antibodies and substrates is an efficient strategy for desirable antibody immobilization.

In this study, rabbit anti-human ferritin (anti-hFT) polyclonal immunoglobulin G (IgG) was chemically co-immobilized with poly(ethylene glycol) (PEG) onto polystyrene submicroparticles (sMPs) for development of sMP/anti-hFT/PEG (SAP) immunolatex. (Scheme 1) To optimize its performance, the effects of immobilization conditions on anti-hFT were evaluated in detail with respect to the degree of immobilization, antigen recognition, and orientation. Electrostatic repulsion between anti-hFT and sMPs at basic pH inhibited anti-hFT access to the sMP surface, but promoted its antigen-accessible orientation on the surface, resulting in high antigen recognition capacity of immobilized anti-hFT (named “soft landing” mechanism). Both the “soft landing” mechanism and subsequent PEGylation, which maintain the co-immobilized antibody’s orientation, are indispensable for constructing a

high-performance SAP immunolatex.

2. Materials and methods

2.1 Materials. Aqueous suspension of carboxylated polystyrene sMPs (10% w/v, without surfactant) [27,28], bovine serum albumin (BSA), rabbit anti-human ferritin (anti-hFT) polyclonal IgG (9.76 mg/mL, pH7.0, isoelectric point (pI) = 6~7), human ferritin (hFT) from spleen, and human sera from patients with rheumatoid arthritis (containing 29 ng/mL rheumatoid factor (RF); lot XI1005) and from healthy persons (without RF) were a kind gift from Biokit S.A. (Barcelona, Spain). According to the manufacturer's data, the surface charge density of the sMPs is 25.67 μC cm^{-2}, and the area occupied by each carboxyl functional group is 62.4 $Å^2$. The particle size (251 nm) and electrophoretic mobility (μ_e = -4.45 μmcm/Vs) of the sMPs in borate buffer solution (10 mM, pH 8) were measured on a Malvern Zetasizer Nano ZS instrument (He-Ne laser, U.K.). α-Methoxy-poly(ethylene glycol)-pentaethylenehexamine (mPEG-N6, M_n = 6000 g/mol; Scheme 1a) [27,28] aqueous solution (2% w/v, pH 10) was provided by JSR Co. (Tokyo, Japan). Unless otherwise stated, mPEG-N6 was always diluted in phosphate buffer (PB, pH 7.4) and 0.01 M HCl to achieve a final concentration of 0.3% w/v (8 mM PB, pH 7.4). 1-Ethyl-3-[3-dimethylaminopropyl]carbodiimide hydrochloride (EDC, special grade) and 2-morpholinoethanesulfonic acid (MES) were provided by Kanto Chemical Co., Inc. (Tokyo, Japan) and Dojindo Laboratories (Kumamoto, Japan), respectively. All buffers used in this

study were prepared from sodium salts, deionized water (Millipore Milli-Q), and 1 M NaOH aqueous solution for pH adjustment. Unless otherwise stated, all experiments were performed at 25ºC or room temperature.

2.2 Methods

2.2.1 Antibody immobilization at different pH levels and salt concentrations.

To estimate the effect of ionic strength by salt addition, low-concentration buffer solutions (ionic strength, I = 0.6 mM) were used in this experiment. As previously reported [27], a stoichiometric amount of EDC aqueous solution (3 μL, 12.5 mg/mL, EDC/COOH of sMPs = 1) was added to a mixture of and sMP suspension (30 μL) and MES buffer (167 μL, 3 mM, pH 5.5) to activate sMP carboxyl groups. The mixture was then shaken for 20 min. The EDC-activated sMPs (30 μL, with active ester groups on the surface) were further diluted with 263 μL of PB (pH 7.4, I = 0.6 mM, containing 0–18 mM NaCl) or borate buffer (pH 8.0–9.5 with the same I and NaCl concentration) to alter the pH and/or salt concentration. Then, freshly diluted anti-hFT in corresponding buffer (9 μL, 1 mg/mL) was fed and incubated for 1 h to allow the immobilization reaction between amine residues and the sMP active ester groups to occur. Low pH (<7.4) was unsuitable for this study.

After anti-hFT immobilization, the sMP/anti-hFT conjugates (sensitized sMPs) were separated by centrifugation (15,000 rpm for 20 min at 25ºC; KR-20000; KUBOTA Co., Tokyo, Japan). A Micro BCA protein assay kit (#23235; Thermo Fisher Scientific Int., IL)

was used to quantify both sMP-bound and free anti-hFT, as previously reported [27].

To measure the reactivity of bound anti-hFT with a high signal-to-noise ratio and to colloidally stabilize the sensitized sMPs for various experiments, the residual bare sMP surfaces after antibody binding were further covered with mPEG-N6 for 30 min to form the sMP/anti-hFT/PEG immunolatex (SAP) through the covalent reaction between multiple mPEG-N6 amine end groups (0.3% w/v in 0.27 mM PB, pH 7.4) and the active ester groups on the surface. In this treatment, the final sMP and mPEG-N6 concentrations were both 0.1% w/v. The SAP immunolatex preparation protocol is illustrated in Scheme 1b. The resulting SAP immunolatex was centrifuged at 60,000 rpm for 20 min at 25ºC (CS 150GX; Hitachi Koki Co. Ltd., Japan) to eliminate unbound antibody in the supernatant, which would otherwise competitively recognize antigens during the reactivity assay. The collected purified SAP immunolatex was homogeneously resuspended in borate buffer (pH 8.0, 10 mM, containing 0.9 g/L NaN_3) by ultrasonication (35 W, 60 Hz, ~20 s for several rounds), followed by storage at 4ºC for 1 day before use. Note that all the SAP immunolatex samples prepared at different pH levels were monodispersed and similar in size (261–268 nm). We did not observe any variations in these properties before and after redispersion prior to reactivity measurements.

On the basis of the results of these experiments, buffer concentrations were optimized and used in the following experiments to enhance buffering capability without promoting

aggregation of sensitized sMPs.

2.2.2. Effects of antibody-binding time.

EDC-activated sMPs (1.24 mL) were diluted in 10.85 mL of borate buffer (buffer A, pH 9.5, 9 mM, I = 6 mM) or PB (pH 7.4, 2.7 mM, I = 6 mM) to alter the pH, followed by addition of freshly diluted anti-hFT dissolved in the same buffer (372 μL, 1 mg/mL) for immobilization. After 1, 5, 10, 20, 30, 60, and 90 min, the suspension (300 μL) was removed and centrifuged (15,000 rpm, 4 min×2 or 10 min×1, 25ºC; KR-20000; KUBOTA Co., Tokyo, Japan) to obtain the supernatant (250 μL), which was used to quantify free antibodies with the Micro BCA assay. Alternatively, the construction and purification of SAP immunolatex for immunoreactivity measurements was carried out as previously described. SAP immunolatex separately prepared at pH 7.4 and pH 9.5 are referred to as SAP(7.4) and SAP(9.5), respectively.

After PEGylation, free anti-hFT content was checked to confirm released antibody after immunolatex formulation. To exclude the contribution from mPEG-N6, which also gave some color in the assay [27], PEGylated EDC-activated sMPs without antibodies were used as a control. This is a reasonable treatment because mPEG-N6 weakly colored the assay and the coupled mPEG-N6 was present at low concentations [27].

2.2.3. Immunoreactivity measurements.

We measured the immunoreactivity of purified SAP immunolatex with an automatic Biokit

Quantex Analyser (BQA 5802–0149; Furuno Electric Co., Ltd., Japan) on the basis of the particle-enhanced immunoagglutination phenomenon. (Scheme 2) Briefly, a given amount of hFT (30 μL, pH 7.0, containing 50 mM Tris, 1 g/L NaN_3, 100 mM NaCl, and 10 g/L BSA) at room temperature was mixed with assay buffer at 8ºC (190 μL, PB buffer, pH 7.4, 10 mM, containing 1 g/L BSA and 0.9 g/L NaN_3) in a cuvette at 37ºC. Then, SAP immunolatex (50 μL, at 8ºC; sMPs concentration: 0.1% w/v) was added in and mixed well immediately. The increment in the absorbance at 570 nm (ΔAbs_{570nm}), which was generated from the rapid agglutination of particles specifically triggered by antibody–antigen recognition, was monitored immediately for ~3 min and defined as the immunolatex immunoreactivity.

2.2.4. Circular dichroism (CD) and fluorescence measurements.

After an original anti-hFT solution was diluted in buffers (I = 6 mM) at different pH levels (pH = 7.4, 8.5, and 9.5), circular dichroism (CD) and fluorescence spectra were monitored every 10 min for 1 h. To avoid pH changes during the assay, the cell was sealed with parafilm. The CD spectra were recorded on a J-720W spectropolarimeter (Jasco, Japan), with a 1-mm quartz cell for far-ultraviolet radiation (260 to 200 nm) and a 10-mm quartz cell for near-ultraviolet radiation (320 to 260 nm) in a temperature-controlled (25ºC) cuvette holder. The anti-hFT concentrations were 0.1 and 1 mg/mL, respectively. The scan speed was 200 nm/min, which was the average of 10 scans for each measurement. The CD spectra were corrected for the buffer blank, and the mean residue ellipticities were calculated using a value

of 110 for the mean residue weight. The fluorescence spectra for anti-hFT were recorded at a concentration of 0.5 mg/mL on an F-7000 fluorometer (Hitachi High-Technologies Co., Japan), with a 1-cm quartz cell in a temperature-controlled (25ºC) cuvette holder. The excitation wavelength was 280 nm, and the emission spectrum was between 290 to 450 nm.

2.2.5. Orientation assay of bound anti-hFT.

The orientation assay of bound anti-hFT was performed on a PL-2500 spectrophotometer (Shimadzu, Japan). Briefly, a given amount of human serum containing 29 ng/mL of RF was poured into PB buffer (pH 7.4, 10 mM) to a final volume of 450 μL. Then, 50 μL of purified SAP immunolatex (sMPs concentration of 0.1% w/v) was added and mixed well, and the absorbance was immediately monitored at a wavelength of 550 nm for 5 min at room temperature. Because RF is an IgM antibody, which comprises multiple units specific for recognizing the Fc region of human and rabbit IgG [29,30], it may agglutinate the SAP immunolatex containing rabbit anti-hFT with the Fc region facing outward, which we term the "head-on" orientation shown in Scheme 3. The absorbance thus increased because of the assembled SAP particles. The higher the absorbance increment (ΔAbs_{550nm}) within a 5 min-period, the more "head-on" orientated bound anti-hFTs the SAP immunolatex has. In a parallel experiment, human serum without RF was used to confirm that RF specifically triggered SAP immunolatex agglutination.

2.2.6. Dynamic light scattering (DLS) and electrophoretic mobility (μ_e) measurements.

A Malvern Zetasizer Nano ZS instrument (He-Ne laser, 633 nm, Worcestershire, U.K.) was used for dynamic light scattering (DLS) and electrophoretic mobility (μ_e) measurements at 25ºC. All test samples were measured after dilution in borate buffer (pH 8.0, 10 mM, I = 0.6 mM) to a final sMP concentration of approximately 2.5×10^{-3}% w/v. Notably, the borate buffer's low ionic strength is a prerequisite for evaluating the variation in μ_e values; otherwise, the surface charge will be thoroughly screened by ions. Each measurement was repeated at least 4 (DLS) or 3 (μ_e) times, and the mean value was reported as the result.

2.2.7. Statistics analysis.

The results shown in this study are all expressed as average ± S.D. (n = 3), except for the CD and fluorescence measurements. P values were calculated based on the t-test analysis.

3. Results

3.1. Antibody immobilization at different pH levels.

To evaluate the effects of pH on antibody immobilization, anti-hFT was chemically bound to sMPs in buffers (I = 0.6 mM without salt) at several pH levels. The amounts of both bound and unbound anti-hFT were then quantified. Figure 1a shows the pH-dependent amounts of free (Γ_f) and bound anti-hFT (Γ_b) in the system before PEGylation, as calculated with the Micro BCA assay. As the Γ_f increased, the Γ_b gradually decreased with increasing pH. These results confirm that high pH values disfavor anti-hFT immobilization, in agreement with the results of previous reports, which show that the maximum amount of adsorbed proteins

appeared at a pH value close to the pI [21,22,25]. After PEGylation to construct the SAP immunolatex, immunoreactivity measurements were performed at a range of antigen concentrations. Figure 1b summarizes the SAP immunolatex immunoreactivity, which reflects the antigen recognition of immobilized anti-hFT. Interestingly, SAP immunolatex immunoreactivity increased with increasing pH, contrary to the Γ_b decrease stated above. For example, the SAP immunoreactivity at pH 9.5 is twice that at pH 7.4 with an hFT concentration of 56 ng/mL, as shown in the insert in Figure 1b.

3.2. Circular dichroism (CD) and fluorescence measurements.

Because proteins, such as antibodies, are susceptible to changes in environments, it is important to confirm structural changes during modification treatment. Both the anti-hFT CD and fluorescence spectra were monitored at 10-min intervals, following the dilution of the original anti-hFT into buffers at different pH levels, similar to the anti-hFT dilution treatment just before antibody immobilization. Figure 2 shows the anti-hFT far-ultraviolet and near-ultraviolet CD spectra, which were recorded immediately after anti-hFT dilution. These CD spectra showed no environment-induced changes even at the 60-min time point (Fig. S1 in Supporting Information). Anti-hFT fluorescence spectra did not vary, regardless of pH and time point (Fig. S2 in Supporting Information). The far- and near-ultraviolet CD are sensitive to variations in secondary and tertiary protein structures, respectively, and fluorescence intensity and maximum wavelength are also suitable indicators of changes in tertiary structure

[31]. These results show that the anti-hFT structure did not change within 60 min at different pH levels.

3.3. Effects of antibody-binding time.

To gain an insight into the high anti-hFT antigen recognition at basic pH, anti-hFT immobilization at a series of binding times was separately carried out at pH 7.4 and 9.5. Figure 3 shows the Γ_b values both before and after PEGylation, which represents the amount of surface antibody after the immobilization reaction (Fig. 3a) and after PEGylation (Fig. 3b). Before PEGylation (Fig. 3a), almost all anti-hFT was bound to sMPs at pH 7.4, which was observed even after 1 min (theoretical Γ_b for complete binding = 29.9 μg/mL), resulting in a nearly constant Γ_b. On the contrary, binding at pH 9.5 proceeded slowly, and free anti-hFT remained after 90 min. These data clearly suggest that the anti-hFT adsorption rate is extremely high at pH 7.4, but low at pH 9.5. After PEGylation (Fig. 3b, theoretical Γ_b for complete binding = 19.9 μg/mL), large amounts of pre-bound anti-hFT were unexpectedly liberated from sMPs, especially those with short binding times (<20 min). Consequently, Γ_b displayed a similar time-dependency at both pH 7.4 and 9.5. Considering the experimental error (see *Materials and methods*), the slight difference in Γ_b between SAP(7.4) and SAP(9.5) was negligible. Release of antibody was triggered by PEGylation because anti-hFT release from sMPs was not observed following addition of PB (pH 7.4, 8 mM) (Fig. S3 in Supporting Information). Probably, a large amount of mPEG-N6 competitively replaced weakly adsorbed

antibodies before their covalent linkage formation, especially the case with short binding time. Figure 4 shows the antigen recognition to bound anti-hFT as a function of the antibody-binding time. The recognition of SAP(9.5) was much higher than that of SAP(7.4), particularly at short binding times and high antigen concentrations. Although the SAP(7.4) and SAP(9.5) Γ_b values increased with time up to 90 min (Figure 3b), we did not observed a significant increase in antigen recognition, especially for SAP prepared with a long antibody-immobilization time. Excessive antibody immobilization [32] has been shown to decrease antigen recognition because of steric restriction. However, in our experiments, the reactivity increased at higher concentrations of immobilized antibody (Fig. S4 in Supporting Information). The different antigen affinities clearly indicate that the amount of immobilization antibody is not responsible for the high SAP(9.5) immunoreactivity.

3.4. Orientation assay of immobilized anti-hFT.

As described in the *Materials and methods*, RF IgM may specifically recognize the anti-hFT Fc region. Therefore, the high ΔAbs_{550nm} value denotes that the SAP immunolatex contains more "head-on" orientated anti-hFT molecules (Scheme 3). Figure 5a shows the SAP(7.4) and SAP(9.5) ΔAbs_{550nm} values, both with an antibody-immobilization time of 20 min, as a function of the volume of RF-containing human serum. Although the 2 values increased with an increase in the RF amount, the ΔAbs_{550nm} value was much higher for SAP(7.4) than for SAP(9.5) under the same conditions. The SAP immunolatex ΔAbs_{550nm}

value obtained with human serum without RF is zero, regardless of the amount of human serum used. The results confirm that RF specifically agglutinated the SAP immunolatex and that SAP(7.4) contained more nonreactive "head-on" orientated anti-hFT than did SAP(9.5). Notably, SAP(7.4) and SAP(9.5) used in this experiment had the same Γ_b (Fig. 3b). Thus, their different ΔAbs_{550nm} values reflect different orientation states of bound anti-hFT. The correlation between the ΔAbs_{550nm} value of SAP immunolatex and the antibody-binding time was then estimated using the same amount of RF (3 μL of RF-containing human serum), and the resultant correlation profiles are summarized in Figure 5b. Unike the ΔAbs_{550nm} of SAP(7.4), which increased immediately after antibody immobilization, the SAP(9.5) ΔAbs_{550nm} increased only at the later time points in the antibody-immobilization experiment, suggesting that a long antibody-binding time tends to cause orientation changes under alkaline conditions. Figure 5c provides the ΔAbs_{550nm} Γ_b-dependency calculated from the results shown in Figures 5b and 3b, for which linear and concave upward Γ_b-dependency curves were separately obtained for SAP(7.4) and SAP(9.5). On the basis of this data, we suggest that the antibody that immobilized under alkaline conditions was probably highly oriented. Its orientation, however, gradually changed during the immobilization process under the same conditions.

3.5. Electrophoretic mobility (μ_e) measurements.

We tested the SAP immunolatex electrophoretic mobility (μ_e) to obtain further information

about the antibody's surface, and we observed some intriguing phenomena. The SAP immunolatex μ_e is presented as a function of the antibody-binding time (Fig. 6a) and of its Γ_b (Fig. 6b). The μ_e value of SAP(9.5) was much higher than that of SAP(7.4) at a binding time of 1 min. However, this value continuously decreased over time in the case of SAP(9.5), while we did not observed a change in the μ_e value of SAP(7.4). Finally, the μ_e values for SAP(7.4) and SAP(9.5) became equal. A rapid decrease in the μ_e value of SAP(9.5) occurred at $\Gamma_b > 10$ μg/mL, accompanied with an invariable μ_e value of SAP(7.4). Proteins tend to change their conformation to spread on the surface after binding with each other to enhance their interaction [14], and adsorption retardation, such as that at pH 9.5, further promoted this tendecy [24]. Because of the conformational changes in the antibody after a prolonged antibody-immobilization phase, the remaining surface might be significantly reduced, thereby restricting subsequent PEGylation and resulting in a decreased μ_e value. We assumed that the relatively low PEGylation effectiveness at neutral pH, in comparison with that at basic pH [33], accounts for the constant low SAP(7.4) μ_e values. Otherwise, a dense PEG layer might efficiently shield the surface charge to give a high μ_e value. Actually, we found that the μ_e values of PEGylated sMPs (sMP/PEG complex) under the same conditions without antibody were –2.4 (at pH 9.5) and –2.7 (at pH 7.4) μm cm/Vs, and both values were almost constant within 60 min. The PEGylation results will be reported elsewhere.

4. Discussion

As described in the *Introduction*, the physisorption properties of anti-hFT might play an important role in its chemical immobilization reaction. On the basis of the sMP surface and anti-hFT (pI = 6 ~ 7) characteristics, the hydrophobic effect and the electrostatic interactions, in particular, are crucial for efficient anti-hFT adsorption. Compelling evidence was obtained from the anti-hFT immobilization at pH 9.5 in the presence of salt (3–9 mM NaCl). Γ_b significantly increased as salt concentration increased, whereas no variation was observed in Γ_b at pH 7.4 under the same conditions (Table S1 in Supporting Information). Salt decreased the electrostatic repulsive force between anionic anti-hFT and the negatively charged sMP surface at high pH, confirming that the electrostatic repulsive force retards the access of the antibody to the sMP surface under alkaline conditions.

Generally, there are three possibilities that may account for increased immunoreactivity: (1) a net increase in antibody's antigen recognition before immobilization, (2) increased antibody immobilization (or antibody-surface concentration), and (3) changes in the orientation of bound antibodies [16,17,26]. With regards to an increase in binding recognition, we evaluated structural variations in anti-hFT in terms of time-dependent circular dichroism (CD) and fluorescence spectra at different pH levels. We did not observe any variation in the anti-hFT structure within 60 min. (Fig. 2) Since the anti-hFT dilution was usually performed less than 5 min before immobilization, the structure of anti-hFT should not have changed significantly. Moreover, the whole SAP immunolatex preparation, including both antibody immobilization

and PEGylation, took place over the course of an hour. Therefore, increased antigen recognition of anti-hFT prior to immobilization seems unlikely. An increased amount of surface antibody is also unlikely because SAP(7.4) and SAP(9.5) had similar Γ_b values despite the difference in the antibody binding time (Fig. 3b). To ascertain whether changes in orientation could account for our results, the orientation of bound anti-hFT was directly analyzed with human serum containing Fc-region-recognizable RF. As shown in Figure 5b, the initial SAP (9.5) ΔAbs_{550nm} value was much lower than that of SAP(7.4) (Γ_b < 10 μg/mL), suggesting the presence of differently oriented immobilized antibodies at pH 7.4 and pH 9.5. As the amount of immobilized antibody increased, however, more SAP(9.5)-derived anti-hFT molecules with Fc regions facing outward gradually appeared on the surface (Fig. 5c), confirming that the increased amount of pre-bound antibody changed the orientation of post-bound one. Moreover, the μ_e values of SAP(9.5) further supported our results. The Γ_b-dependent μ_e value (Fig. 6b) and ΔAbs_{550nm} (Fig. 5b) of SAP(9.5) were mostly constant at Γ_b < 10 μg/mL before continuous variation.

On the basis of these results, it is plausible that the differences in immunoreactivity between SAP(7.4) and SAP(9.5) originated from different orientations of bound anti-hFT. At pH 7.4, almost neutral anti-hFT might strongly prefer hydrophobic attractions with sMPs, resulting in an extremely rapid or instant adsorption process and random orientation (Scheme 4a). The enhanced electrostatic repulsive force at pH 9.5 compensated for the hydrophobic

interaction, retarding anti-hFT adsorption onto the negatively charged surface. In principle, IgG adsorption preferentially occurs with its Fc region on the hydrophobic surface, owing to its hydrophobic characteristics and/or the structural instability over the IgG antigen-binding region ($F(ab')_2$) [24]. Additionally, the anti-hFT $F(ab')_2$ region (pI = ~5.6) [34] should be negatively charged at high pH and electrostatically repelled from sMPs. Thus, retardation of anti-hFT adsorption may provide time for anti-hFT orientation changes, such as the change to the "end-on" orientation (Fc region close to the surface as shown in Scheme 3), which favor antibody-antigen recognition (Scheme 4b). We named this the "soft landing" mechanism. It should be emphasized here that subsequent PEGylation played a key role in maintaining the immobilized antibody's orientation, as reported previously [13]. However, this situation changed as the amount of surface antibody increased, probably because of weakened repulsive forces, leading to randomly oriented bound antibody similar to that found at pH 7.4. In addition, the pre-bond antibodies might also change orientation and/or conformation at longer antibody-binding times before PEGylation, thus losing antigen recognition [13]. Consequently, SAP(9.5) showed higher antigen recognition than SAP(7.4), but both values remained constant at later time points. (Fig. 4)

5. Conclusion

By physically manipulating anti-hFT orientation during chemical immobilization, we successfully formed a high-performance SAP immunolatex. The detailed study on anti-hFT

immobilization with respect to the extent of immobilization, antigen recognition, and anti-hFT orientation, supports the idea of a rapid blocking effect of PEGylation following short-term antibody immobilization. This effect benefited from the combination of physical adsorption and covalent binding of antibodies. Physical adsorption may have resulted in facile orientation changes and covalent binding may have anchored antibodies robustly, unlike traditional time-consuming antibody immobilization protocols. Moreover, the consistency of the Γ_b-dependent variations in antibody orientation and the SAP immunolatex μ_e values implies that electrophoretic mobility measurements probably provide a convenient indirect approach to investigate antibody orientation, which relies on the inherent structural nature of the antibody/PEG hybrid layer on sMPs. It should be mentioned here that the proper pH level for obtaining proper antibody orientation may be adjusted down to close to antibody's PI by using highly charged sMPs, if antibodies are not stable enough at high pH level during the binding process. Thus, although more experiments are still required, the "soft landing" mechanism proposed in this study seems a general rule for antibody binding and will attract more attention as a useful tool in the near future.

Acknowledgments: This research was supported by Biokit S.A. (Barcelona, Spain) and a Grant-in-Aid for Scientific Research on Innovative Areas (Soft Interface # 20106011) from the Ministry of Education, Culture, Sports, Science and Technology (MEXT) of Japan.

Appendix A. Supplementary data

Supplementary data associated with this article can be found, in the online version, at

References

[1] S. K. Mwilu, A. O. Aluoch, S. Miller, P. Wong, O. A. Sadik, Anal. Chem. 81 (2009) 7561.

[2] M. B. Sosellner, K. A. Dickson, B. L. Nilsson, R. T. Raines, J. Am. Chem. Soc. 125 (2003) 11790.

[3] T. Cha, A. Guo, X. Zhu, Proteomics 5 (2005) 416.

[4] A. Watzke, M. Kohn, M. Gutierrez-Rodriguez, R. Wacker, H. Schroder, R. Breinbauer, J. Kuhlmann, K. Alexandrov, C. M. Niemeyer, R. S. Goody, H. Waldmann, Angew. Chem. Int. Ed. 45 (2006) 1408.

[5] Z. Suo, X. Yang, R. Avci, M. Deliorman, P. Rugheimer, D. W. Pascual, Y. Idzerda, Anal. Chem. 81(2009) 7571.

[6] H. Chon, S. Lee, S. W. Son, C. H. Oh, J. Choo, Anal. Chem. 81(2009) 3029.

[7] Y. Nagasaki, H. Kobayashi, Y. Katsytana, T. Jomura, T. Sakura, J. Colloid Interface Sci. 309 (2007) 524.

[8] T. Tanaka, T. Matsunaga, Anal. Chem. 72 (2000) 3518.

[9] J. M. Peula, R. Hidalgo-Alvarez, F. J. de las Nieves, J. Colloid Interface Sci. 201(1998) 132.

[10] P. Peluso, D. S. Wilson, D. Do, H. Tran, M. Venkatasubbaiah, D. Quincy, B. Heidecker, K. Poindexter, N. Tolani, M. Phelan, K. Witte, L. S. Jung, P. Wagner, S. Nock, Anal. Biochem. 312 (2003) 113.

[11] J. W. Chung, J. M. Park, R. Bernhardt, J. C. Pyun, J. Biotechnol. 126 (2006) 325.

[12] A. A. Karyakin, G. V. Presnova, M. Y. Rubtsova, A. M. Egorov, Anal. Chem. 72 (2000) 3805.

[13] K. Yoshimoto, M. Nishio, Y. Nagasaki, J. Am. Chem. Soc. 132 (2010) 7982.

[14] P. Lin, S. Chen, K. Wang, M. Chem, A. K. Adak J. Hwu, Y. Chen, C. Lin, Anal. Chem. 81 (2009) 8774.

[15] J. D. Conradie, M. Govender, L. Visser, J. Immunol. Methods 59 (1983) 289.

[16] I. N. Chang, J. N. Lin, J. D. Andrade, J. N. Herron, J. Colloid Interface Sci. 174 (1995) 10.

[17] R. van-Erp, Y. E. M. Linders, A. P. G. van-Sommeren, T. C. Gribnau, J. Immunol. Methods 152 (1992) 191.

[18] Y. Yuan, H. He, L. J. Lee, Biotechnol. Bioeng. 102 (2009) 891.

[19] Y. Jung. J. M. Lee, H. Jung, B. H. Chung, Anal. Chem. 79 (2007) 6534.

[20] H. Shen, J. Watanantibodye, M. Akashi, Anal. Chem. 81 (2009) 6923.

[21] J. L. Ortega-Vinuesa, M. J. Galvez-Ruiz, R. Hidalgo-Alvarez, Langmuir 12 (1996) 3211.

[22] J. Buijs, J. W. T. Lichtenbelt, W. Norde, J. Lyklema, Colloids Surf. B 5 (1995) 11.

[23] J. Zhou, H. Tsao, Y. Sheng, S. Jiang, J. Chem. Phys. 121 (2004) 1050.

[24] J. Buijs, W. Norde, Langmuir 12 (1996) 1605.

[25] S. Chen, L. Liu, J. Zhou, S. Jiang, Langmuir 19 (2003) 2859.

[26] J. N. Lin, J. D. Andrade, I. N. Chang, J. Immonol. Methods 125 (1989) 67.

[27] X. Yuan, K. Yoshimoto, Y. Nagasaki, Anal. Chem. 81 (2009) 1549.

[28] X. Yuan, D. Fabregat, K. Yoshimoto, Y. Nagasaki, Anal. Chem. 81 (2009) 10097.

[29] I. Giaever, C. R. Keese, R. I. Rynes, Clin. Chem. 30 (1984) 880.

[30] Y. Hashimoto, T. Ikenaga, Y. Tanigawa, T. Ueda, I. Ezaki, T. Imoto, Biol. Pharm. Bull. 23 (2000) 941.

[31] Y. Tsybovsky, D. V. Shubenok, Z. I. Kravchuk, S. P. Martsev, Protein Eng. Des. Sel 20 (2007) 481.

[32] J. Buijs, D. D. White, W. Norde, Colloids Surf. B 8 (1997) 239.

[33] Information from Biokit S.A.

[34] N. Nakajima, Y. Ikada, Bioconjugate Chem. 6 (1995) 123.

Figure Captions

Scheme 1. (a) Chemical structure of mPEG-N6 and (b) SAP immunolatex construction.

Scheme 2. Schematic representation of the immunoreactivity assay used in this study.

Scheme 3. Schematic illustration of the specific interaction between rheumatoid factor (RF) and the Fc region of bound anti-hFT.

Scheme 4. Proposed mechanism of anti-hFT immobilization at (a) pH7.4 and (b) pH9.5.

Figure 1. (a) pH-dependent antibody amount of immobilized anti-hFT (Γ_b, ●) and free anti-hFT (Γ_f, ○) in the system before PEGylation measured by Micro BCA assay. (b) Immunoreactivity of SAP immunolatex as a function of hFT concentration (left) and pH-dependent immunoreactivity of SAP immunolatex measured at hFT = 56 ng/mL (right). The SAP immunolatex was prepared by immobilizing anti-hFT at pH7.4 (◇), pH8 (△), pH8.5 (□), pH9 (○), and pH9.5 (×), respectively. ∗ and # : $P < 0.001$ separately vs. that at pH7.4 ; ×: $P < 0.05$ vs. that at pH8.0; +: $P < 0.05$ vs. that at pH8.5 based on t-test analysis (n = 3).

Figure 2. (a) Far-ultraviolet and (b) near-ultraviolet CD spectra recorded immediately (holding time t = 0) after dilution of anti-hFT in buffers at different pH levels. Solid line (—), dotted line (….), and broken line (----) represent the spectra of anti-hFT in a buffer (I = 6 mM) of pH = 7.4, 8.5, and 9.5, respectively.

Figure 3. (a) Time-dependent anti-hFT quantities of sensitized sMPs before PEGylation, and its fraction of the total ($\Gamma_b/(\Gamma_b+\Gamma_f)$), as antibody binding was performed at pH7.4 (△) and pH9.5 (○), respectively. (b) Time-dependent anti-hFT quantities and its fraction of the total ($\Gamma_b/(\Gamma_b+\Gamma_f)$) after the construction of SAP(7.4) (△) and SAP(9.5) (○), respectively. (n= 3)

Figure 4. Correlation between anti-hFT binding time and SAP(7.4) (a) and SAP(9.5) (b) immunoreactivity, respectively. Immunoreactivity measurements were performed at hFT

concentrations of 11 (△ and ▲), 22 (◇ and ◆), and 56 ng/mL (○ and ●), respectively. $*_1$, $\#_1$, and $+_1$: $P < 0.01$ separately vs. that of SAP(7.4) with antibody binding time = 1 min; $*_2$, $\#_2$, and $+_2$: $P < 0.05$ separately vs. that of SAP(9.5) with antibody binding time = 1 min, both based on t-test analysis (n = 3).

Figure 5. (a) Variations in the ΔAbs_{550nm} value of SAP immunolatex (anti-hFT binding time = 20 min) with human serum containing RF (open symbol) or not (close symbol); (b) Antibody-binding time dependent variations in SAP immunolatex ΔAbs_{550nm}; (c) Γ_b-dependent ΔAbs_{550nm} of SAP immunolatex. SAP(9.5) (○ and ●) ; SAP(7.4) (△ and ▲). (n= 3)

Figure 6. (a) Antibody-binding time dependent variations in electrophoretic mobility (μ_e) of SAP immunolatex. (b) Γ_b-dependent SAP immunolatex μ_e. SAP(7.4) (△);SAP(9.5) (○). (n= 3)

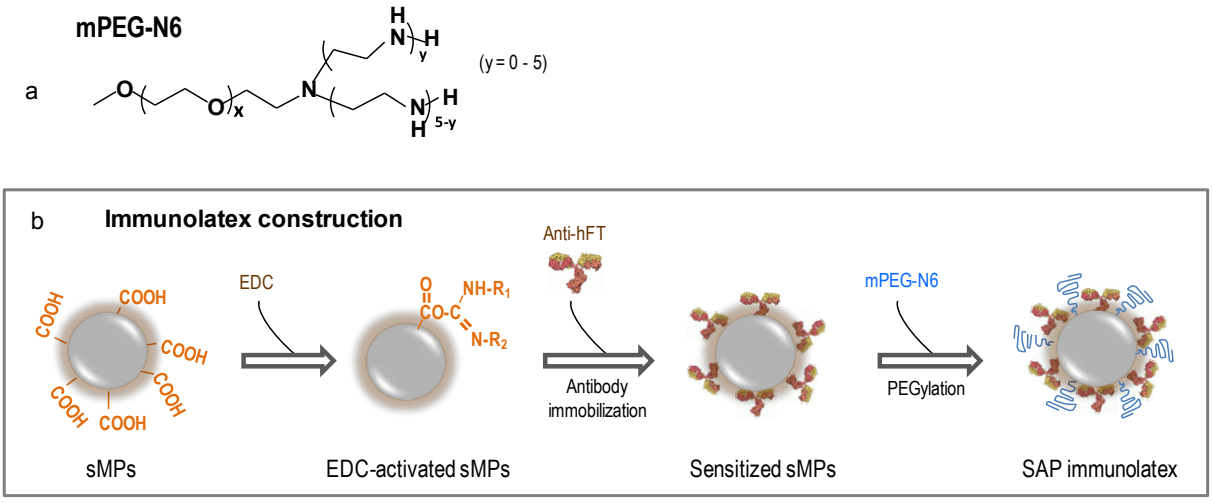
a
mPEG-N6
(y = 0 - 5)
b
Immunolatex construction
EDC
Anti-hFT
Antibody immobilization
mPEG-N6
PEGylation
sMPs
EDC-activated sMPs
Sensitized sMPs
SAP immunolatex

Scheme 1

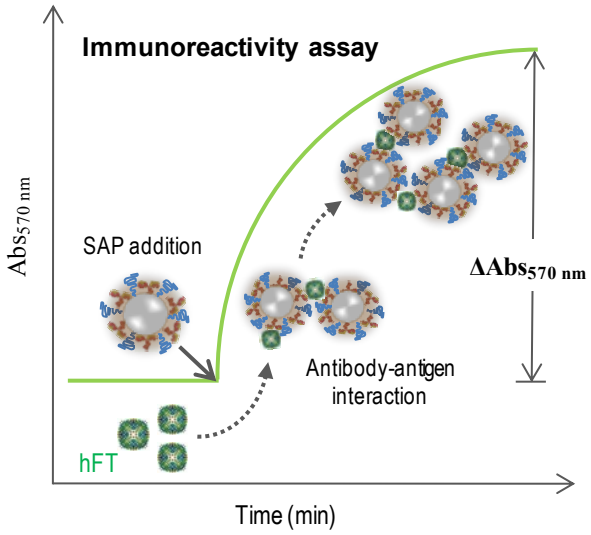
Immunoreactivity assay
Abs570 nm
SAP addition
ΔAbs570 nm
Antibody-antigen
interaction
hFT
Time (min)

Scheme 2

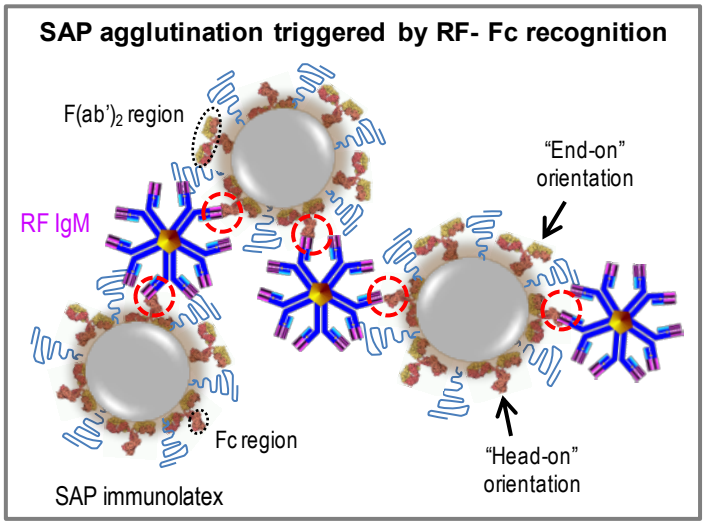
SAP agglutination triggered by RF- Fc recognition
F(ab')2 region
RF IgM
"End-on" orientation
Fc region
"Head-on" orientation
SAP immunolatex

Scheme 3

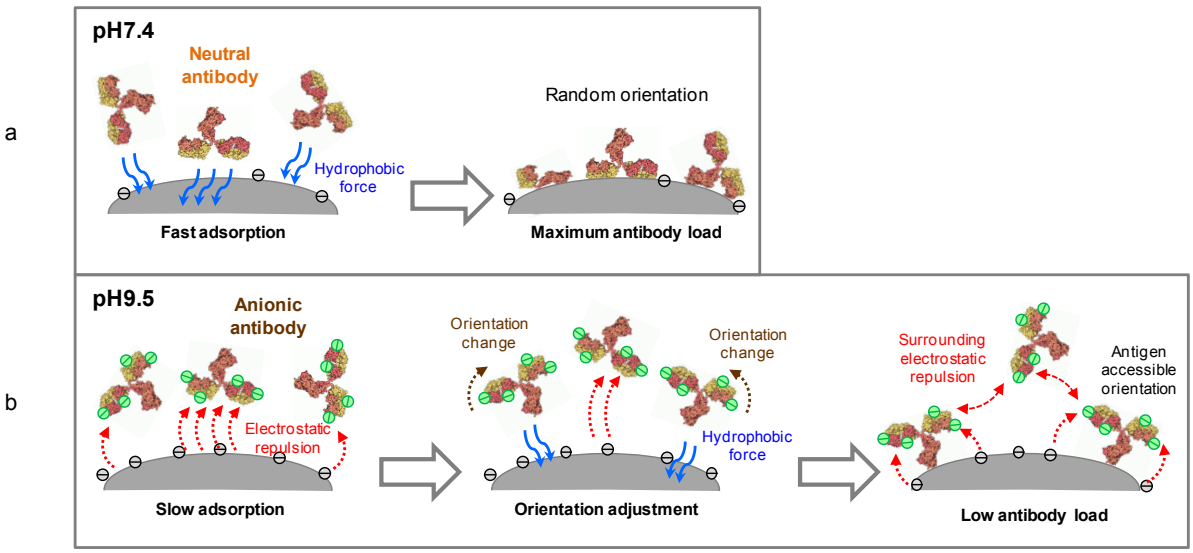
a
pH7.4
Neutral antibody
Hydrophobic force
Fast adsorption
Random orientation
Maximum antibody load
b
pH9.5
Anionic antibody
Electrostatic repulsion
Slow adsorption
Orientation change
Orientation change
Hydrophobic force
Orientation adjustment
Surrounding electrostatic repulsion
Antigen accessible orientation
Low antibody load

Scheme 4

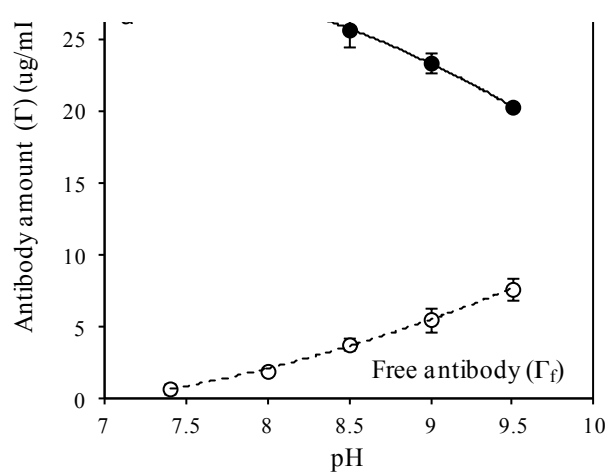
Antibody amount (Γ) (ug/ml
25
20
15
10
5
0
Free antibody (Γ_f)
7
7.5
8
8.5
9
9.5
10
pH

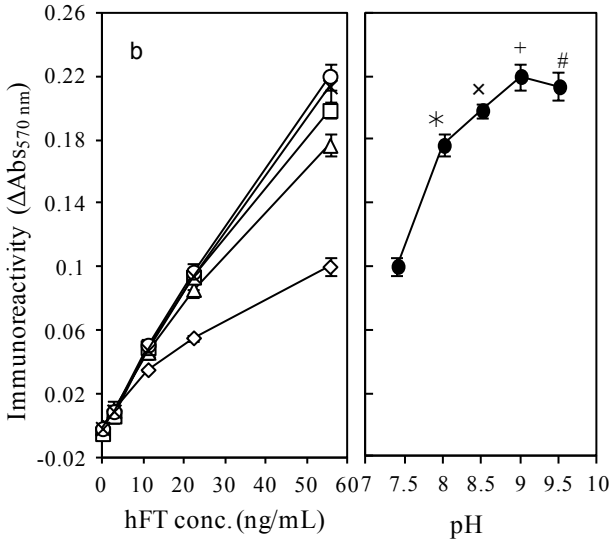
Immunoreactivity ($\Delta Abs_{570\ nm}$)
0.26
0.22
0.18
0.14
0.1
0.06
0.02
-0.02
b
0
10
20
30
40
50
60
hFT conc. (ng/mL)
7
7.5
8
8.5
9
9.5
10
pH
*
×
+
#

Figure 1

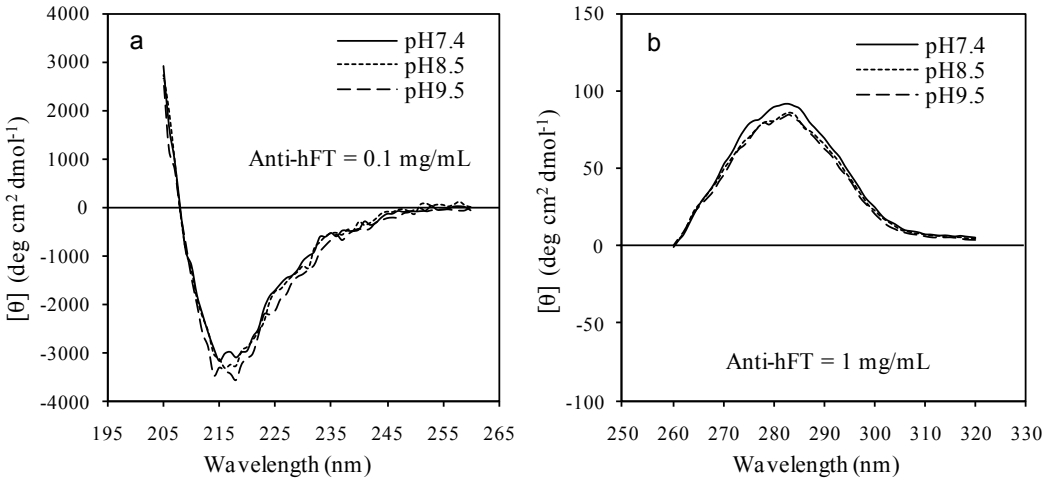
a
pH7.4
pH8.5
pH9.5
Anti-hFT = 0.1 mg/mL
[θ] (deg cm2 dmol-1)
Wavelength (nm)
b
pH7.4
pH8.5
pH9.5
Anti-hFT = 1 mg/mL
[θ] (deg cm2 dmol-1)
Wavelength (nm)

Figure 2

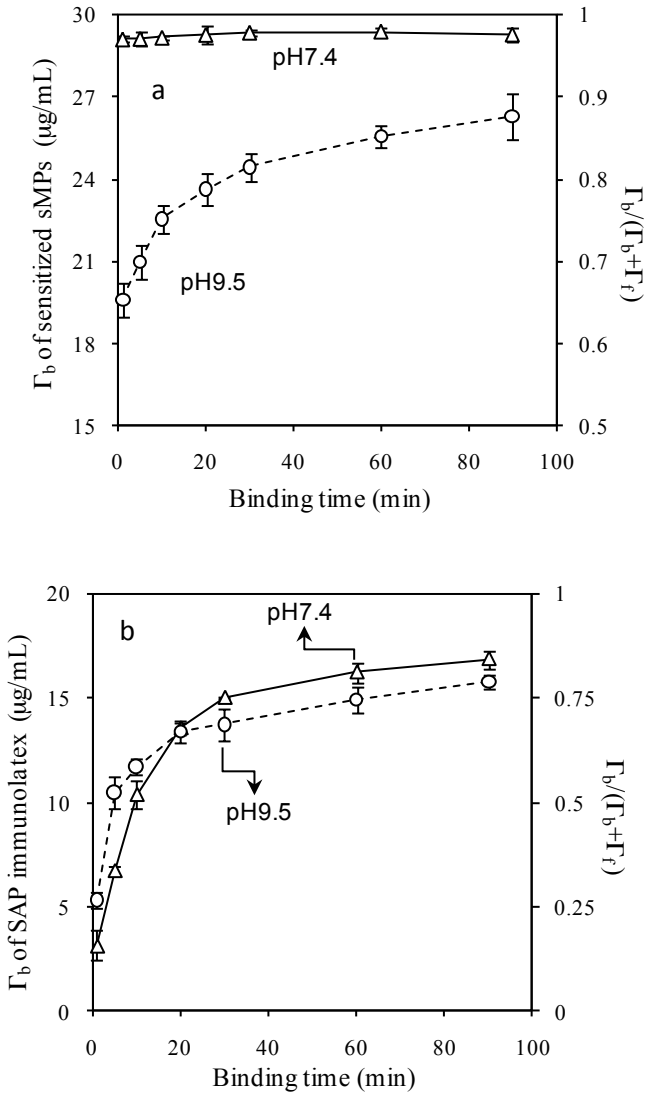
a
pH7.4
pH9.5
Γb of sensitized sMPs (μg/mL)
Γb/(Γb+Γf)
Binding time (min)
b
pH7.4
pH9.5
Γb of SAP immunolatex (μg/mL)
Γb/(Γb+Γf)
Binding time (min)

Figure 3

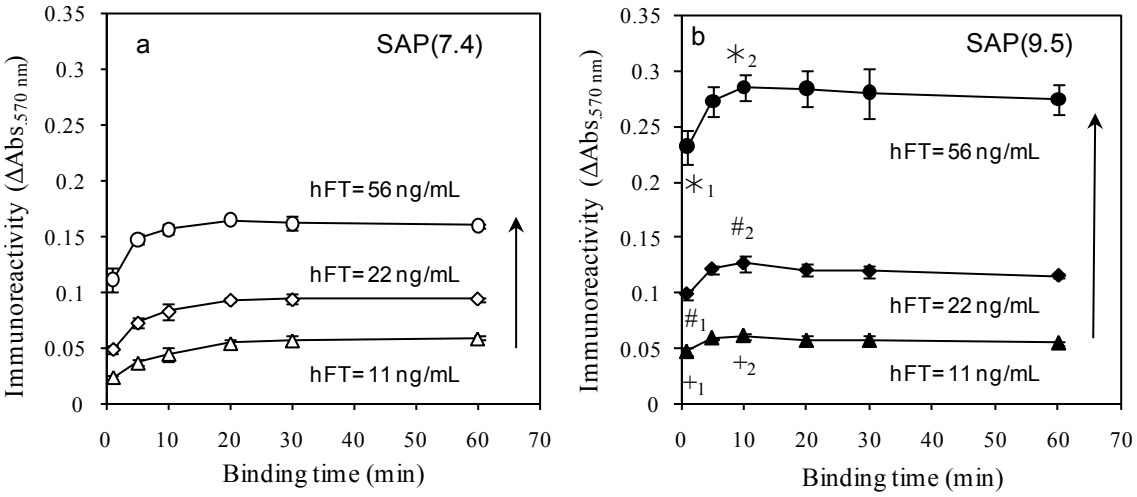
a
SAP(7.4)
hFT= 56 ng/mL
hFT= 22 ng/mL
hFT= 11 ng/mL
Immunoreactivity (ΔAbs570 nm)
Binding time (min)
b
SAP(9.5)
hFT= 56 ng/mL
hFT= 22 ng/mL
hFT= 11 ng/mL
Immunoreactivity (ΔAbs570 nm)
Binding time (min)

Figure 4

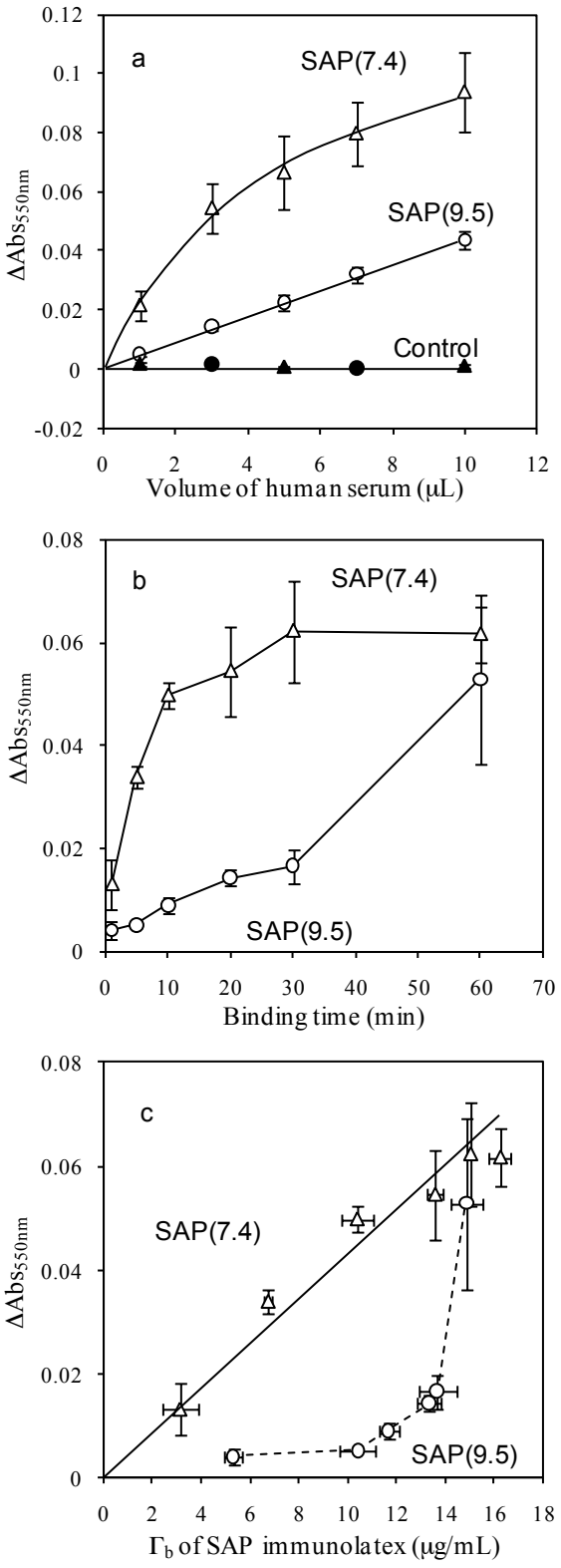
a
SAP(7.4)
SAP(9.5)
Control
ΔAbs550nm
Volume of human serum (μL)
b
SAP(7.4)
SAP(9.5)
ΔAbs550nm
Binding time (min)
c
SAP(7.4)
SAP(9.5)
ΔAbs550nm
Γb of SAP immunolatex (μg/mL)

Figure 5

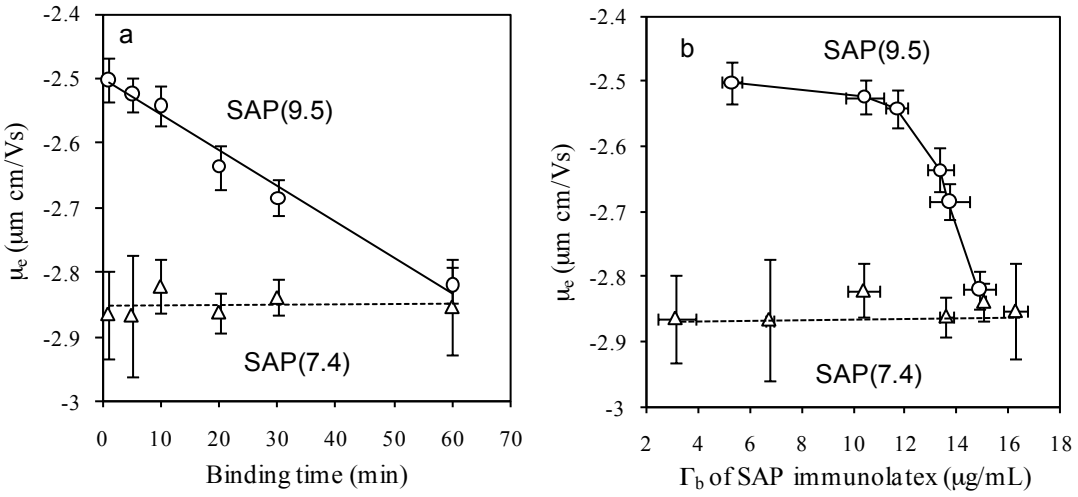
a
SAP(9.5)
SAP(7.4)
μe (μm cm/Vs)
Binding time (min)
b
SAP(9.5)
SAP(7.4)
μe (μm cm/Vs)
Γb of SAP immunolatex (μg/mL)

Figure 6